BMC Oral Health

RESEARCH Open Access

Effect of occlusal splint design and thickness on temporomandibular joint loading: a finite element study

Başak Topdağı[1*], Elifnur Güzelce Sultanoğlu[1], Alanur Çiftçi Şişman[2], Hüsna Aktürk[3] and Kübra Karaosmanoğlu[4]

Abstract

Objectives Occlusal splints are a mainstay in the management of temporomandibular disorders, but the mechanical influence of design and thickness variations on joint and dental structures remains unclear. This study compared the stress and strain distributions within the temporomandibular joint (TMJ) and adjacent tissues produced by Michigan (stabilization) and non-permissive splints of 3-mm and 5-mm thicknesses using finite element analysis.

Materials and methods Three-dimensional models of the maxilla, mandible, teeth, periodontal ligament, and articular disc were reconstructed from the Visible Human Project dataset. Michigan and non-permissive splints were modeled with occlusal thicknesses of 3 mm and 5 mm. Functional muscle forces were applied to simulate mandibular movements, and linear static analyses were performed in OptiStruct under defined boundary conditions.

Results The splint-free model showed the highest stress levels in all structures. Non-permissive splints significantly reduced mandibular stress (32.3 MPa) but increased loading on the periodontal ligament. Michigan splints resulted in lower periodontal ligament stresses and a more even stress distribution within the articular disc. Increasing splint thickness improved stress reduction only in the non-permissive model.

Conclusions Occlusal splints lowered peak stresses in the TMJ and related structures. Non-permissive splints provided greater joint protection, while Michigan splints achieved a more balanced distribution of occlusal forces.

Clinical relevance Splint design and thickness affect how loads are transferred through the temporomandibular system. Non-permissive splints, particularly at 5 mm, reduced joint stress but increased periodontal ligament loading. Splint selection should consider the main treatment goal, with attention to using the minimal effective thickness.

Keywords Occlusal Splints, Temporomandibular joint disorders, Finite element analysis, Stress, Mechanical

*Correspondence:
Başak Topdağı
basak.topdagi@sbu.edu.tr
[1]Department of Prosthodontics, Hamidiye Faculty of Dentistry, University of Health Sciences, Istanbul, Türkiye, Turkey
[2]Department of Oral and Maxillofacial Surgery, Hamidiye Faculty of Dentistry, University of Health Sciences, Istanbul, Turkey
[3]Department of Oral and Maxillofacial Surgery, Faculty of Dentistry, Istun Universty, Istanbul, Turkey
[4]Department of Restorative Dentistry, Faculty of Dentistry, Ankara University, Ankara, Turkey

Introduction

Temporomandibular disorders (TMDs) are common clinical conditions characterized by pain, functional limitations, and structural alterations within the temporomandibular joint (TMJ) and its associated components [1, 2]. Their etiology is multifactorial and has been associated with parafunctional habits, trauma, occlusal factors, and psychosocial stressors [3, 4]. The increasing levels of stress and the adverse lifestyle changes associated with modern life have led to a rise in the prevalence of TMDs and, consequently, an increased need for treatment [5, 6]. Occlusal splints are conservative, reversible, and non-invasive treatment options that are commonly used to reduce joint loading, alleviate muscle hyperactivity, and protect the teeth [7, 8]. Previous studies have reported that the use of splints in the management of TMDs is a highly effective and critical treatment modality [2, 9]. However, the effects of different splint designs and thicknesses on the biomechanics of the TMJ have not yet been fully elucidated [10, 11].

Occlusal splints can be fabricated in various designs, such as stabilization (Michigan), non-permissive, and anterior repositioning types, and can be applied in different thicknesses [12–16]. These parameters may alter mandibular positioning and occlusal contacts, thereby influencing the distribution of intra-articular stresses [17, 18]. There is a general consensus in the literature that hard acrylic resin remains the material of choice for occlusal splints, as its mechanical properties contribute significantly to their clinical performance [19, 20]. In contrast to the consensus regarding material selection, there is no similar consensus regarding splint type or thickness; in clinical practice, these parameters are largely determined by the clinician's preference, and biomechanical evidence on this matter remains limited [4, 18, 21, 22].

Finite element analysis (FEA) is a valid method that enables the investigation of stress and strain distribution within the TMJ and its associated structures under controlled loading conditions [8, 23]. Although several FEA studies have investigated mandibular biomechanics and occlusal appliances, comprehensive analyses evaluating the combined effect of splint design and thickness on TMJ biomechanics remain limited [8, 24–26]. The complex structure of the TMJ, patients' tendency toward irregular appliance use, and the confounding effects of additional interventions such as botulinum toxin or combined therapies make clinical investigations difficult and complicate the independent interpretation of results [25, 27].

The aim of this study was to investigate the effects of different occlusal splint designs and thicknesses on stress and strain distribution within the TMJ using three-dimensional finite element analysis. Accordingly, three hypotheses were proposed. First, the presence of a splint was expected to reduce stress and strain values in the mandible and TMJ structures compared with the no-splint model. Second, Michigan-type splints, which allow a certain degree of mandibular mobility, were hypothesized to reduce TMJ stress more effectively than movement-restrictive non-permissive splints. Third, thicker occlusal splints were hypothesized to be more effective than thinner splints in reducing stress within the TMJ tissues.

Materials and methods

This study was approved by the Non-Interventional Clinical Research Ethics Committee of the University of Health Sciences, Hamidiye Campus (Date: May 15, 2025; Decision No: 11/33; Project Registration No: 25/444).

Modeling of cortical bone, trabecular bone, and teeth

Three-dimensional finite element models were created and analyzed on HP workstations equipped with 2.40 GHz Intel Xeon E-2286 processors and 64 GB ECC RAM. Anatomical data for bone and teeth were obtained from the open-access *Visible Human Project* (U.S. National Library of Medicine) [28]. Three-dimensional finite element models were created and analyzed on HP workstations equipped with 2.40 GHz Intel Xeon E-2286 processors and 64 GB ECC RAM. Anatomical data for bone and teeth were obtained from the open-access *Visible Human Project* (U.S. National Library of Medicine) [28]. Tomographic datasets were processed in 3D Slicer and converted to STL format, then reconstructed into three-dimensional models using Blender. Mesh optimization was performed in Altair HyperMesh, and finite element analyses were conducted using the Altair OptiStruct solver.

Tomographic data were segmented and reconstructed into three-dimensional anatomical models. The cortical and trabecular structures of the maxilla and mandible were defined by applying an inward offset, and all components were spatially aligned for simulation. Rotational mandibular movements were assigned for each experimental condition: natural occlusion was simulated in the no-splint model, whereas mandibular rotation angles of 3° and 5° were applied to represent functional positions with 3-mm and 5-mm splints, respectively (Fig. 1).

Modeling of splint types, periodontal ligament, articular disc, and working models

In this study, non-permissive and Michigan-type splint models were designed in three dimensions using Blender software, with a thickness of 0.8 mm in the buccal and lingual regions, and either 3–5 mm on the occlusal surfaces. These thicknesses were selected based on commonly reported clinical fabrication ranges, as previous clinical and imaging studies have investigated splint thicknesses

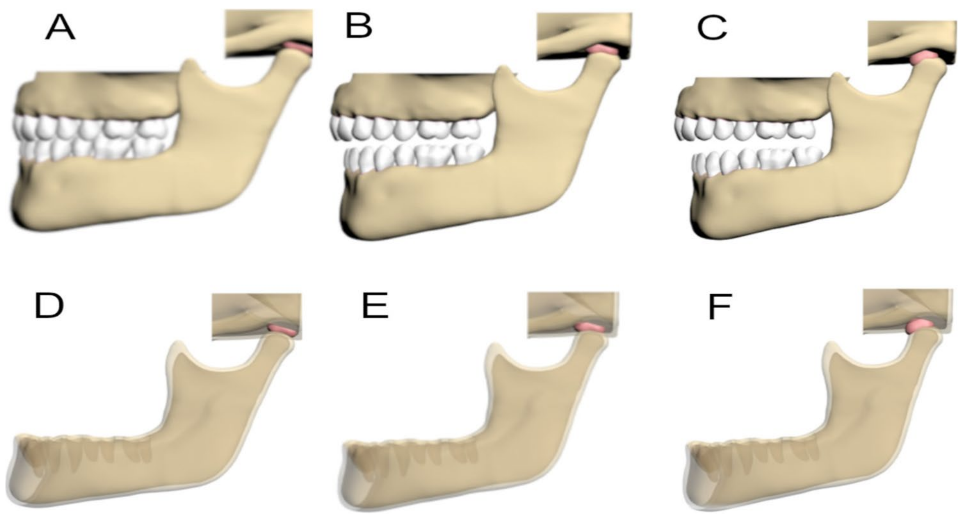

Fig. 1 Three-dimensional reconstruction and segmentation workflow used for cortical bone, trabecular bone, and dental structures. Anatomical datasets from the Visible Human Project were processed in 3D Slicer, converted to STL format, and refined in Blender to generate the maxillary and mandibular bone models. Inward offset was applied to distinguish cortical and trabecular layers, and rotational mandibular movements were simulated for each condition. **A** Dental occlusion in natural occlusion without splint. **B** Dental occlusion with 3-mm splint condition. **C** Dental occlusion with 5-mm splint condition. **D** Disc position in natural occlusion without splint. **E** Disc position with 3-mm splint condition. **F** Disc position with 5-mm splint condition. This workflow ensured anatomically accurate modeling and standardized mandibular positioning across all experimental conditions

Table 1 Models and abbreviations used in the study

Model code	Definition
NS	Full occlusion without splint (ICM)
NP3	Non-permissive splint, 3 mm thickness
NP5	Non-permissive splint, 5 mm thickness
M3	Michigan splint, 3 mm thickness
M5	Michigan splint, 5 mm thickness

between 3 and 6 mm [13, 26]The nomenclature and design specifications for each analyzed model are presented in Table 1; Fig. 2. The periodontal ligaments were modeled with a uniform thickness of 0.25 mm around the roots of each tooth, based on the outer surfaces of the maxillary and mandibular teeth. The contact area between the articular disc and the condyle was adjusted depending on the splint thickness. In the absence of a splint (full occlusion), the disc was positioned over the posterior region of the condyle with an approximate contact area of 39.24 mm^2. When a 3 mm-thick splint was applied, the interaction zone shifted toward the middle-anterior region, reaching approximately 57 mm^2. At 5 mm splint thickness, the contact area expanded to include both anterior and middle regions, with a total area of approximately 83 mm^2 [29, 30]. To ensure accurate load transfer between components, mesh conformity was achieved using Altair HyperMesh.

Material properties and model generation

All components were assumed to be linearly elastic and isotropic. Each component was defined by its elastic modulus (E) and Poisson's ratio (ν) to simulate mechanical behavior (Table 2). Geometries created in Blender were transferred to HyperMesh, where appropriate surface and solid meshing was applied. The models were analyzed using the OptiStruct solver, and mesh independence was confirmed through a convergence test. Detailed mesh parameters are provided in the Supplementary File (Supplementary File.).

Loading scenarios and boundary conditions

In all models, muscle forces associated with functional mandibular movements were applied in anatomically appropriate directions and magnitudes (Table 3). To prevent stress singularities, forces were distributed across adjacent nodes. The models were fixed by constraining the degrees of freedom at selected nodes in the superior maxillary bone region. A freeze-type contact was defined between interacting components to ensure coordinated surface movement during deformation. Under these loading and boundary conditions, a total of twenty linear static analyses were performed across five models (Fig. 3).

Results

Finite element analyses demonstrated that splint thickness, surface characteristics, and loading direction substantially influenced the stress and strain distribution within the mandibular complex. The maximum von Mises stress and strain values obtained from each model are summarized in (Tables 4, 5 and 6), (Figs. 4, 5, 6, 7, 8, 9, 10, 11, 12, 13, 14, 15, 16, 17, 18).

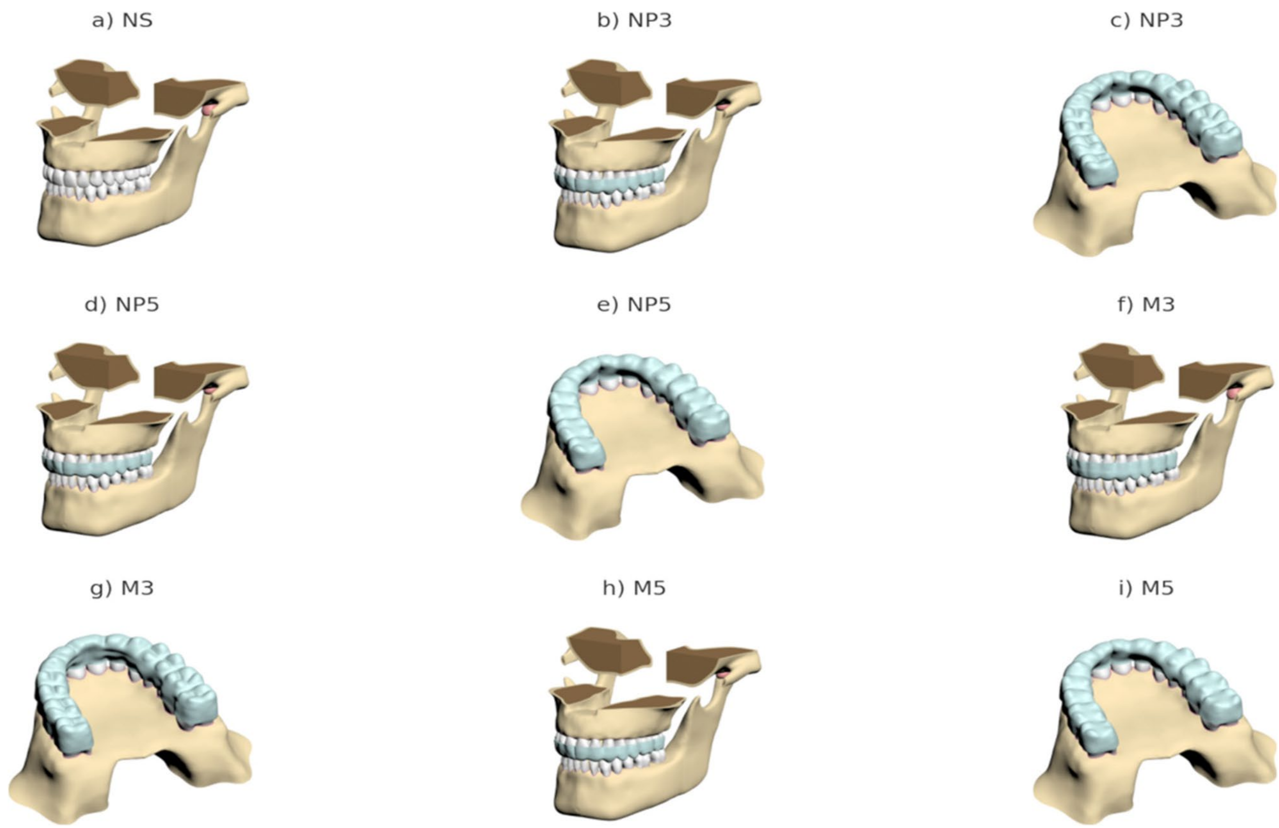

Fig. 2 Three-dimensional modeling of Michigan-type and non-permissive occlusal splints, periodontal ligament, and articular disc. Splints were designed in Blender with 0.8 mm buccolingual and 3–5 mm occlusal thickness. The contact area between the disc and condyle increased progressively from 39.24 mm^2 (no splint) to 57 mm^2 (3 mm splint) and 83 mm^2 (5 mm splint), indicating enhanced load-distribution capacity with increasing splint thickness. The final working models were meshed in Altair HyperMesh to ensure load-transfer accuracy and node conformity

Table 2 Mechanical properties of the materials used in the finite element analysis

Material	Elastic Modulus (Mpa)	Poisson's Ratio	Reference
Cortical bone (mandibular bone)	13.700	0,30	[23, 31]
Trabecular bone (maxillary bone)	1.370	0,30	[23, 31]
Periodontal ligament	0,07	0,45	[23, 31]
Occlusal splint	3.000	0,45	[23, 31]
Articular disc	2,1	0,49	[23, 31]
Enamel	80.000	0.33	[23, 31]
Dentin	18.600	0.31	[23, 31]

In all models, the highest stress values were generally observed in full closure movement, followed by lateral and protrusive movements. The highest stress and strain values in the mandible, TMJ, and PDL were observed in the NS models in the control group (Fig. 4). When splinted models were evaluated, the highest stress value in the mandible was observed in the NP3 model (37.228 MPa) with full closure movement (Fig. 8). The lowest stress value was observed in the NP5 model (2.695 MPa) with lateral movement (Fig. 9).

Table 3 Direction and magnitude of muscle forces applied in functional movements

Functional movement	Muscle	Angle (°)	Force (*N*)	References
Maximum intercuspation	Temporalis	60	427.7	[32]
	Masseter	15	376.0	[32]
	Medial pterygoid	120	207.6	[32]
	Lateral pterygoid	120	37.3	[32]
Right laterotrusion	Right lateral pterygoid	120	15	[32]
	Left lateral pterygoid	120	10	[32]
Left laterotrusion	Right lateral pterygoid	120	10	[32]
	Left lateral pterygoid	120	15	[32]
Protrusion	Right lateral pterygoid	120	18	[32]
	Left lateral pterygoid	120	18	[32]

When the stress values in the splint were examined according to the splint models, the highest stress values were observed in NP5 for all movements: full closure (65.737 MPa), lateral (3.701 MPa), and protrusive (4.164 MPa), (Figs. 10, 9 and 7). The lowest stress values in the splint were observed in the NP3 model (37.434 MPa) with full closure movement (Fig. 8). Lateral (0.103 MPa) and protrusive (1.814 MPa) movements were observed in M3 models (Figs. 11 and 12).

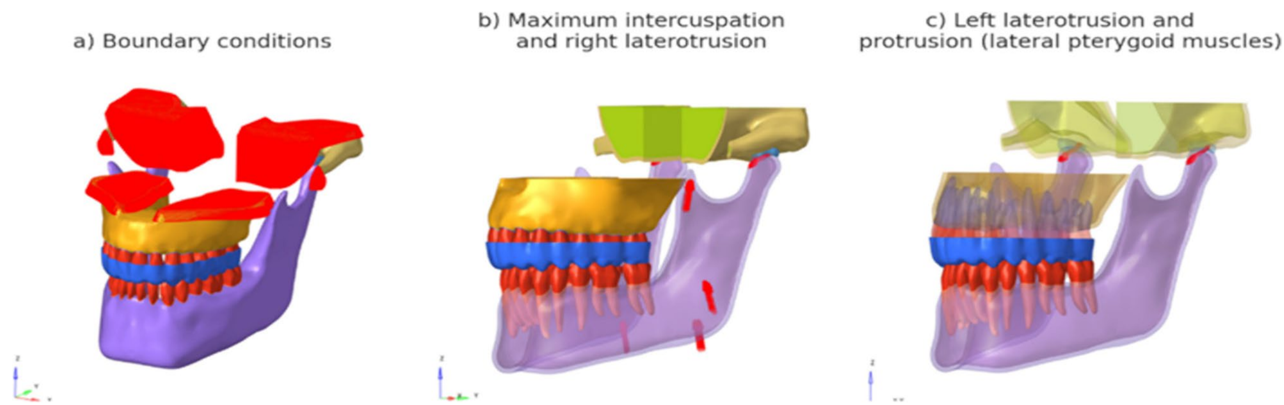

Fig. 3 Finite element analysis workflow illustrating mesh generation, loading vectors, and boundary constraints. Anatomical forces representing functional mandibular movements were applied in physiologic directions and magnitudes, while fixed boundary conditions were defined at the superior maxillary bone. A freeze-type contact ensured synchronized surface deformation, and twenty linear static analyses were performed across the five experimental models. This standardized simulation framework enabled consistent biomechanical comparison among all experimental conditions

Table 4 Maximum von Mises stress (MPa) and strain values in different anatomical regions according to splint design, thickness full closure movement type

Model	Movement type	Mandible stress (MPa)	Mandible strain	Splint stress (MPa)	Splint strain	TMJ disc stress (MPa)	TMJ disc strain	PDL stress (MPa)
NS	Full closure	42.54	2.69E−03	–	–	8.909	4.214	4
M3	Full closure	35.01	2.22E−03	52.69	1.581E−02	7.419	3.509	1.38
NP3	Full closure	37.228	2.355E−03	37.434	1.123E−02	7.127	3.342	3.371
M5	Full closure	35.009	2.215E−03	52.689	1.581E−02	7.419	3.509	1.475
NP5	Full closure	32.310	2.044E−03	65.737	1.972E−02	7.066	3.342	1.655

Table 5 Maximum von Mises stress (MPa) and strain values in different anatomical regions according to splint design, thickness lateral movement type

Model	Movement type	Mandible stress (MPa)	Mandible strain	Splint stress (MPa)	Splint strain	TMJ disc stress (MPa)	TMJ disc strain	PDL stress (MPa)
NS	Lateral movement	3.42	2.16E−04	–	–	0.120	0.057	0.045
M3	Lateral movement	3.24	2.05E−04	0.103	0.40E−04	0.094	0.044	0.021
NP3	Lateral movement	3.21	2.03E−04	3.17	9.52E−04	0.072	0.034	0.030
M5	Lateral movement	2.856	1.81E−04	1.543	4.63E−04	0.094	0.044	0.034
NP5	Lateral movement	2.695	1.71E−04	3.701	1.11E−03	0.062	0.029	0.037

Table 6 Maximum von Mises stress (MPa) and strain values in different anatomical regions according to splint design, thickness protrusion movement type

Model	Movement type	Mandible stress (MPa)	Mandible strain	Splint stress (MPa)	Splint strain	TMJ disc stress (MPa)	TMJ disc strain	PDL stress (MPa)
NS	Protrusion	4.037	2.554E−04	–	–	0.128	0.060	0.054
M3	Protrusion	3.841	2.430E−04	1.814	5.441E−04	0.112	0.053	0.033
NP3	Protrusion	3.79	2.39E−04	3.642	1.008E−04	0.081	0.039	0.039
M5	Protrusion	3.474	2.198E−04	1.818	5.453E−04	0.101	0.048	0.043
NP5	Protrusion	3.424	2.166E-04	4.164	1.2483-04	0.077	0.036	0.045

When the stress values in the TMJ were examined according to splinted models, equal values were observed in M3 and M5 in full closer and lateral movements (Figs. 13, 14, 11 and 15). The highest value was observed in M3 during protrusive movement (Fig. 12). The highest stress value in the TMJ was 7.491 MPa in the full closure M3 and M5 models (Figs. 13 and 8). The lowest stress values observed in the TMJ were observed in the NP5 models in protrusive (0.077 MPa), full closure (7.066 MPa) and lateral movements (0.062 MPa), (Figs. 10, 9 and 7).

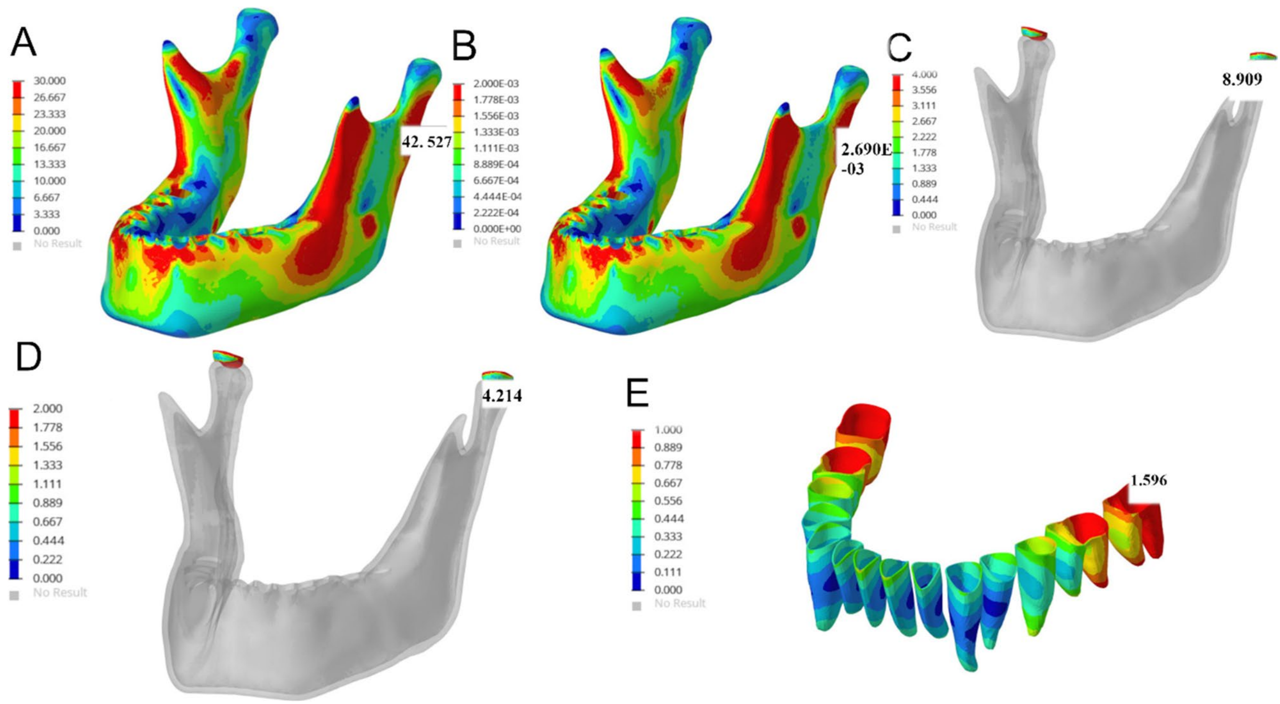

Fig. 4 Finite element analysis of the splint-free (NS) model during intercuspal position (ICM). Mandibular von Mises stress and strain distributions (**a**, **b**), articular disc stress distribution (**c**), and PDL stress concentration pattern illustrating baseline loading prior to splint application (**d**, **e**). The splint-free model exhibited the highest stress concentrations across all evaluated structures, thereby serving as the reference condition for subsequent comparative analyses

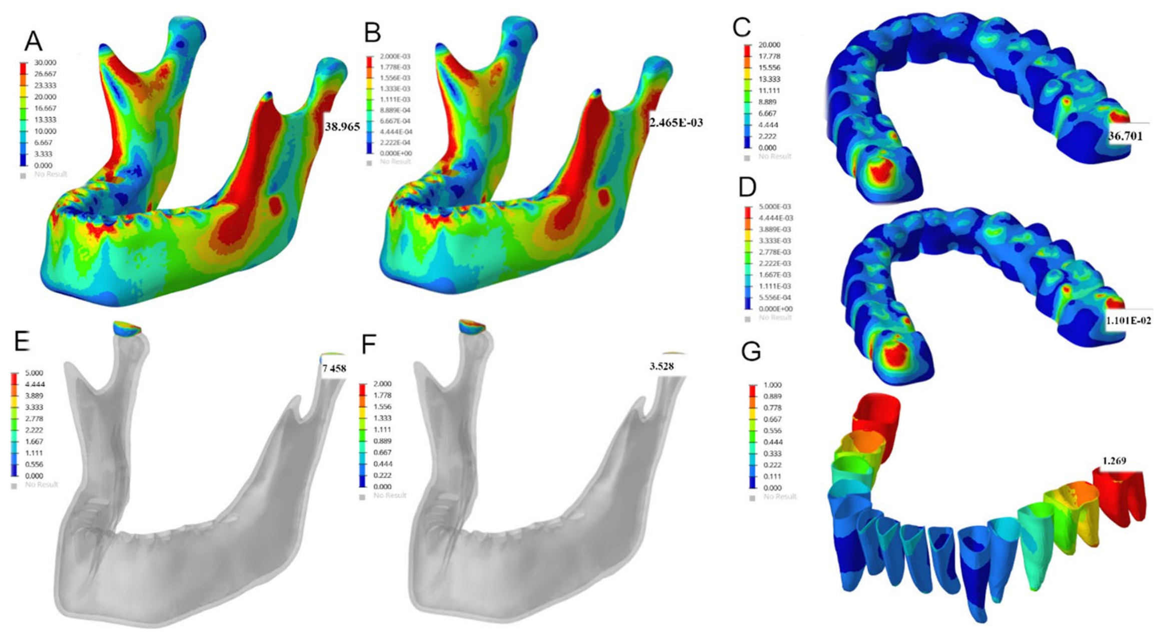

Fig. 5 Stress and strain distributions of the 3-mm Michigan-type splint (M3) model were evaluated under the intercuspal position. Mandibular von Mises stress and strain distributions are presented in (**a**, **b**). Stress and strain within the splint material, predominantly concentrated in the posterior occlusal contact regions, are shown in (**c**, **d**). The articular disc exhibits a more homogeneous, superiorly distributed stress and strain pattern (**e**, **f**), while the maximum periodontal ligament (PDL) stress distribution is illustrated in (**g**).Compared with the splint-free condition, the Michigan-type splint reduced mandibular stress levels and promoted a more uniform distribution of loading across the articular disc. This effect can be attributed to the redistribution of occlusal forces over a broader contact area, thereby decreasing localized stress concentrations in critical anatomical structures

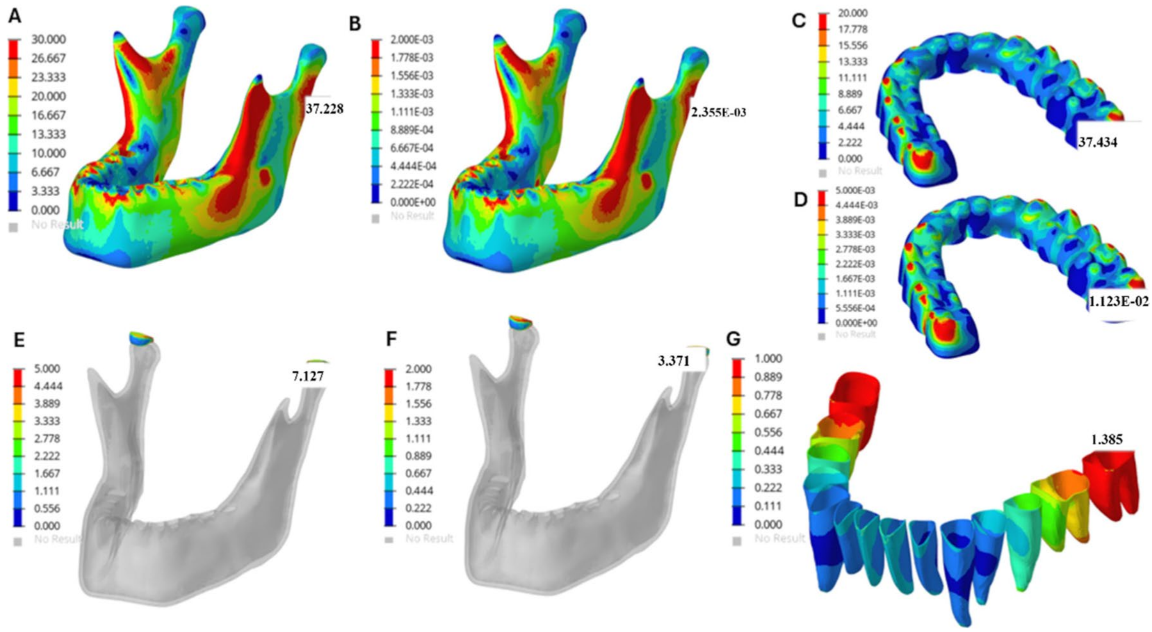

Fig. 6 Stress and strain distributions in the 3-mm non-permissive splint (NP3) model were evaluated under the intercuspal position. Mandibular von Mises stress and strain distributions, showing concentration in the ramus and condylar neck regions, are presented in (**a**, **b**). Stress and strain within the splint material are illustrated in (**c**, **d**). The articular disc demonstrates a stress and strain pattern extending from the posterior region toward the antero-superior aspect (**e**, **f**), while the periodontal ligament (PDL) stress distribution is shown in (**g**).Compared with the splint-free condition, mandibular stress levels were reduced; however, they remained higher than those observed in the Michigan splint model. Additionally, articular disc loading exhibited a more anterior extension, indicating a less uniform stress distribution pattern relative to the permissive splint design

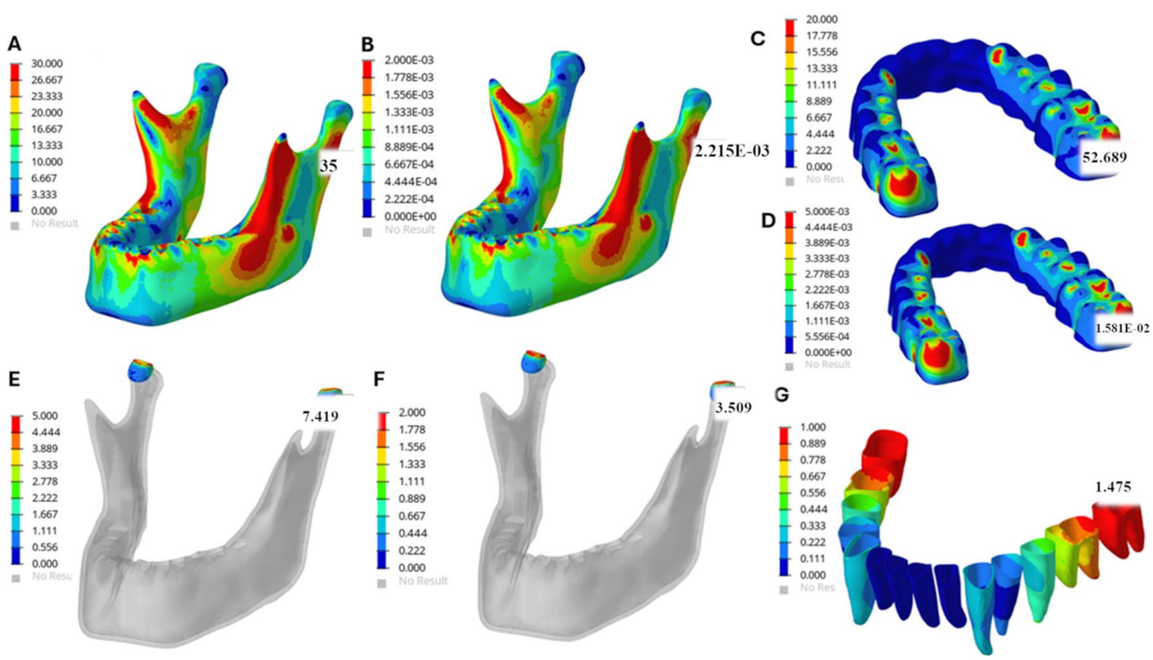

Fig. 7 Stress and strain patterns in the 5-mm Michigan-type splint (M5) model were evaluated under the intercuspal position. Mandibular von Mises stress and strain distributions are presented in (**a**, **b**), while stress and strain within the splint material are shown in (**c**, **d**). The articular disc exhibits stress and strain predominantly concentrated in the posterior region (**e**, **f**), and the periodontal ligament (PDL) demonstrates reduced loading compared with the splint-free condition (**g**).Both mandibular and articular disc stress levels were markedly lower than those observed in the splint-free model. However, increasing splint thickness beyond 3 mm did not result in a substantial additional reduction in stress, suggesting a limited incremental biomechanical benefit with greater splint thickness

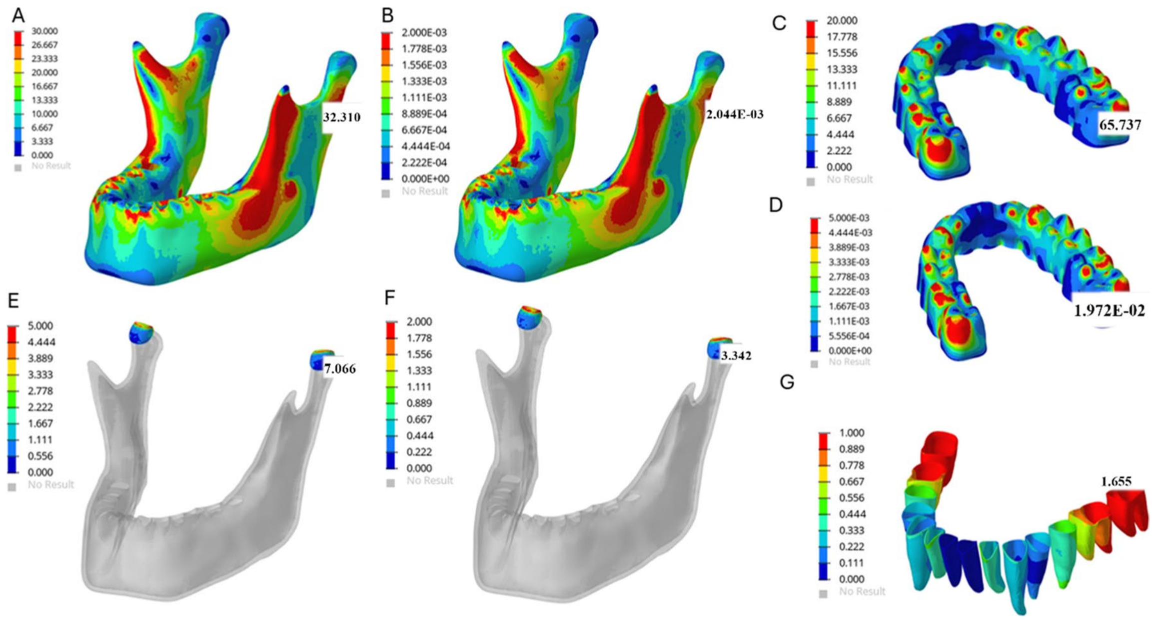

Fig. 8 Stress and strain distributions in the 5-mm non-permissive splint (NP5) model were evaluated under the intercuspal position. Mandibular von Mises stress and strain distributions are presented in (**a**, **b**). Stress and strain within the splint material, predominantly concentrated in the posterior occlusal contact regions, are shown in (**c**, **d**). The articular disc exhibits a stress and strain pattern extending from the posterosuperior toward the anterosuperior region (**e**, **f**), while the periodontal ligament (PDL) stress distribution is illustrated in (**g**). The NP5 configuration yielded the lowest mandibular stress levels among all evaluated models. Additionally, it demonstrated an anterior redistribution of articular disc loading, shifting stress away from primary osseous contact regions and suggesting an altered load transfer mechanism compared with other splint designs

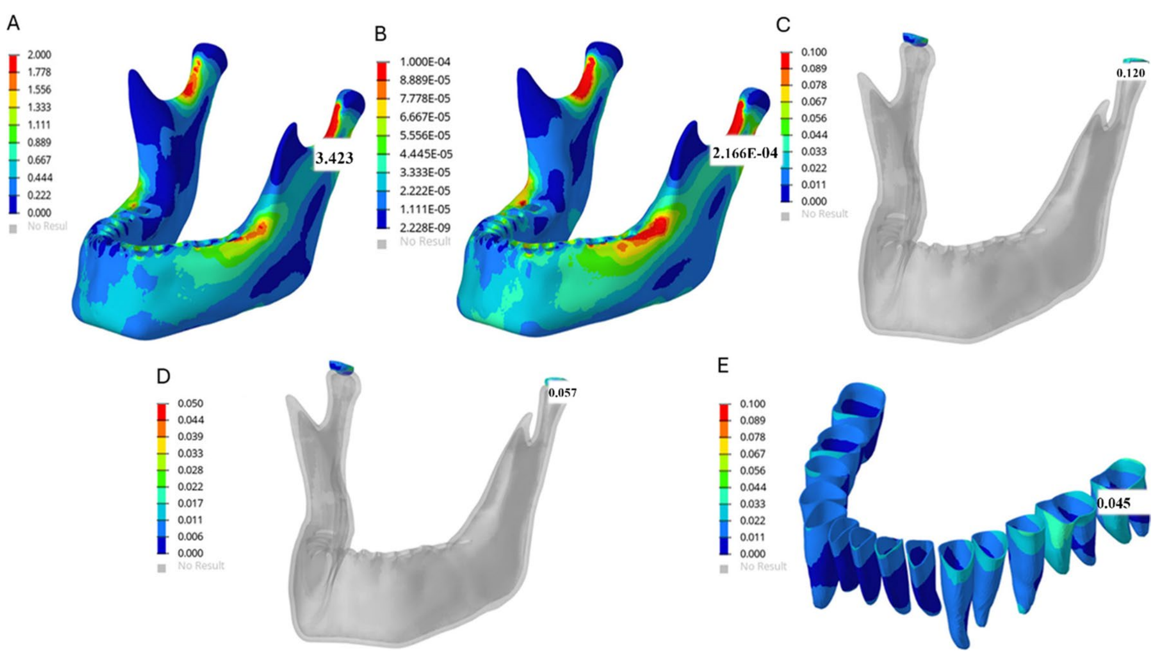

Fig. 9 Lateral excursion in the splint-free (NS) model was evaluated to characterize the baseline biomechanical response under non-assisted conditions. Mandibular von Mises stress and strain distributions, concentrated primarily around the mandibular angle and condylar neck, are presented in (**a**, **b**). The articular disc exhibits stress and strain predominantly in the posterior region (**c**, **d**), while periodontal ligament (PDL) stress concentrations are observed along the posterior root surfaces (**e**). This model represents the baseline lateral loading pattern and serves as the reference condition for comparison with splint-assisted configurations

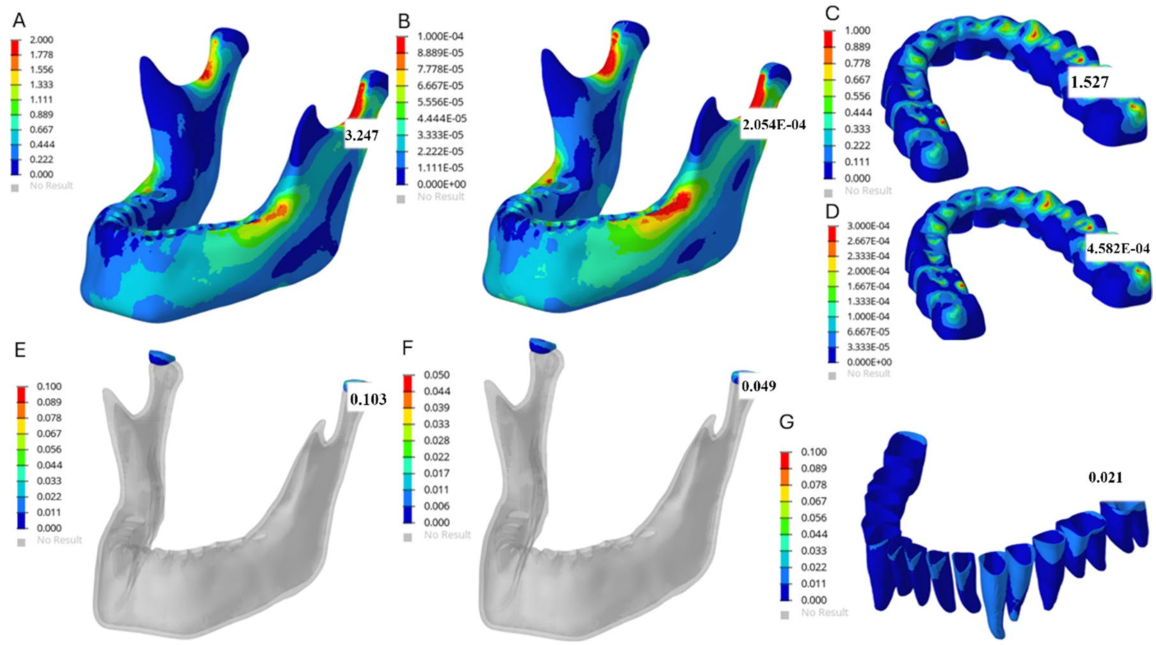

Fig. 10 Lateral excursion in the 3-mm Michigan-type splint (M3) model was evaluated to assess its biomechanical influence under guided occlusion. Mandibular stress and strain distributions are presented in (**a**, **b**). The articular disc exhibits reduced stress and strain intensity compared with the splint-free (NS) model (**c**, **d**), while the periodontal ligament (PDL) demonstrates a more homogeneous stress distribution (**e**). Strain within the splint material is illustrated in (**f**) Compared with the splint-free condition, the M3 splint reduced stress levels in the mandible, articular disc, and periodontal ligament during lateral movement, while promoting a more balanced and evenly distributed loading pattern and posterior root surfaces illustriated in (**g**)

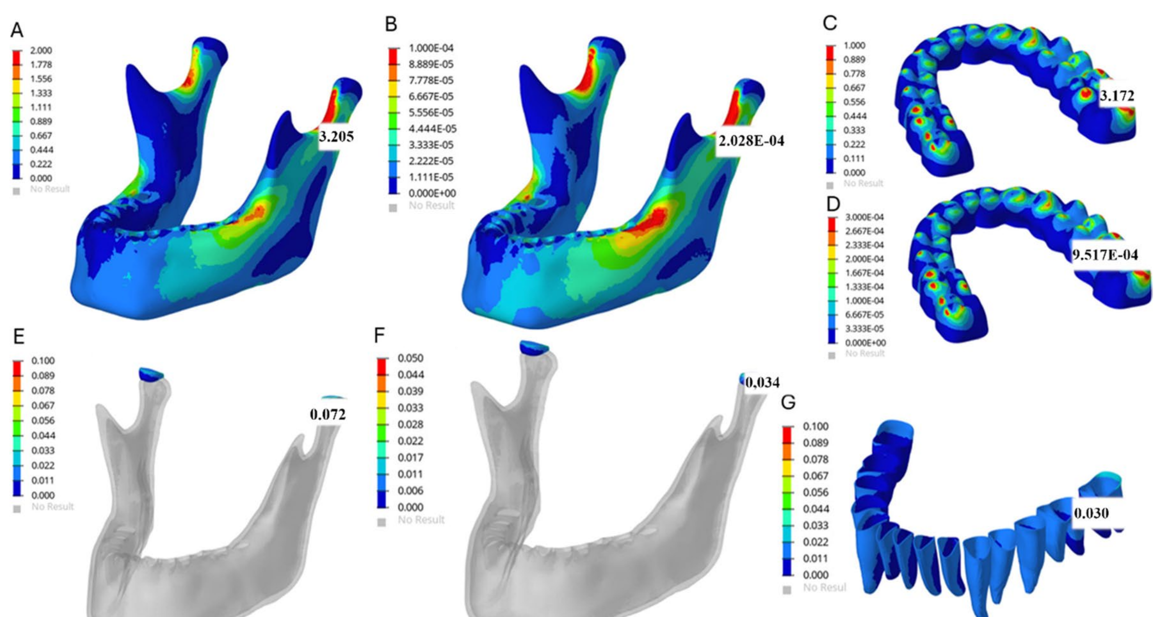

Fig. 11 Lateral excursion in the 3-mm non-permissive splint (NP3) model was evaluated to assess its biomechanical behavior under guided occlusion. Mandibular von Mises stress and strain distributions are presented in (**a**, **b**). Stress and strain within the splint material, predominantly concentrated in the posterior contact regions, are shown in (**c**, **d**). The articular disc exhibits stress and strain primarily localized in the posterosuperior zone (**e**, **f**), while the periodontal ligament (PDL) stress distribution is illustrated in (**g**). Compared with the splint-free condition, the NP3 splint reduced mandibular stress levels; however, loading remained more posteriorly concentrated, and PDL stress levels were higher than those observed in the Michigan splint model. These findings indicate a less favorable stress distribution pattern relative to the permissive splint design during lateral movement

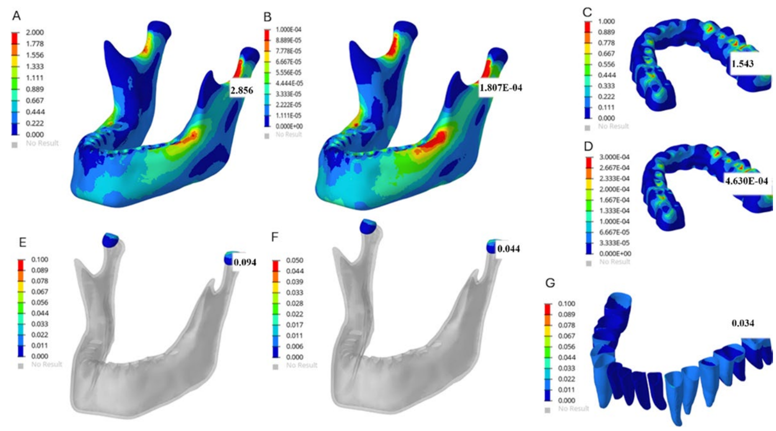

Fig. 12 Lateral excursion in the 5-mm Michigan-type splint (M5) model was evaluated to assess biomechanical responses under guided occlusion. Mandibular stress and strain distributions are presented in (**a**, **b**), and stress and strain within the splint material are shown in (**c**, **d**). The articular disc exhibits predominantly posterior stress and strain (**e**, **f**), while the periodontal ligament (PDL) stress distribution is illustrated in (**g**). The M5 splint further reduced mandibular stress during lateral movement; however, articular disc and PDL stress levels were slightly higher compared with the 3-mm Michigan-type splint configurations, suggesting limited additional benefit from increased splint thickness in these structures

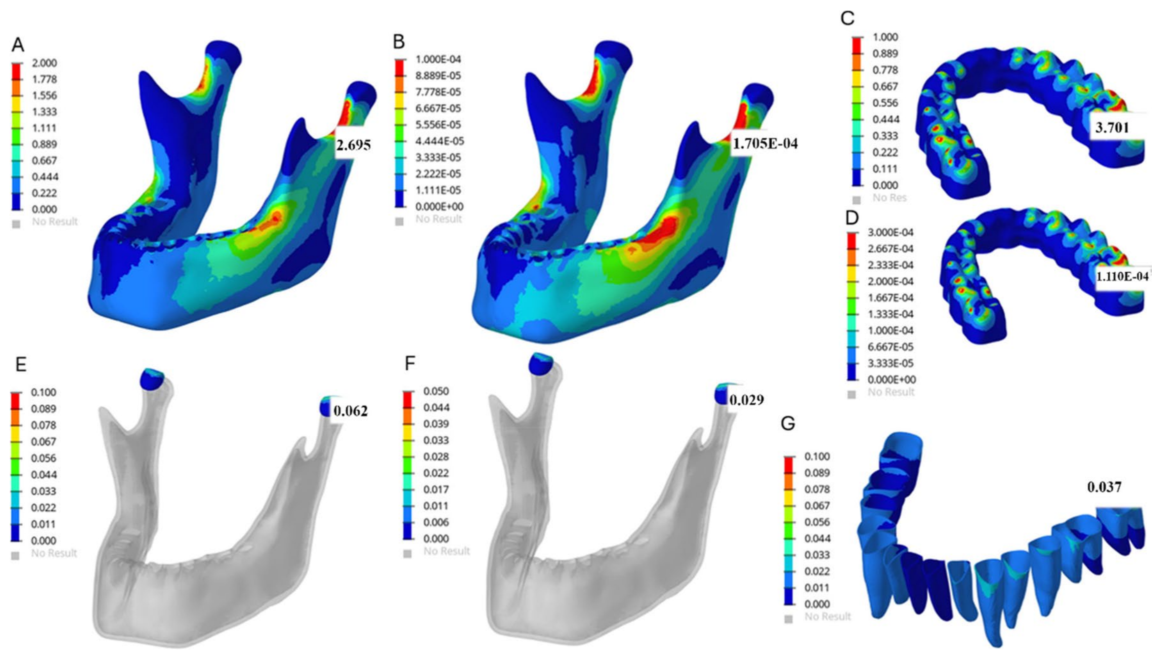

Fig. 13 Lateral excursion in the 5-mm non-permissive splint (NP5) model was evaluated to characterize its biomechanical behavior under guided occlusion. Mandibular von Mises stress and strain distributions are shown in (**a**, **b**), while stress and strain on the splint surface, predominantly localized in posterior regions, are presented in (**c**, **d**). The articular disc exhibits stress and strain concentrated in the posterior region without an anterosuperior shift (**e**, **f**), and the periodontal ligament (PDL) stress distribution is illustrated in (**g**). The NP5 configuration produced the lowest mandibular stress levels during lateral movement. Disc loading remained limited, with stress predominantly concentrated posteriorly, indicating that this splint design effectively reduces mandibular load but maintains a posteriorly focused distribution pattern

The highest stress values in the TMJ disc were observed in full closure movement (3.509 MPa) and lateral movement (0.044 MPa) in M3 and M5, equally (Figs. 13, 14, 11 and 15); the highest stress values in the TMJ disc were observed in NP5 during protrusive movement (0.036 MPa), (Fig. 7). The lowest stress values in the TMJ disc were observed in NP3 and NP5 with equal values during full closure movement (3.342 MPa), (Figs. 8 and 10); and in NP5 during protrusive (0.036 MPa) and lateral (0.029 MPa) movements (Figs. 9 and 7). The highest stress values in the PDL were observed in NP5 during lateral (0.037 MPa) and protrusive (0.045 MPa) movements (Figs. 9 and 7); and in NP3 during full closure movement (3.371 MPa), (Fig. 10). The value in NP3 during full closure movement is the highest value in the PDL (Fig. 10). The lowest stress values in the PDL were observed in

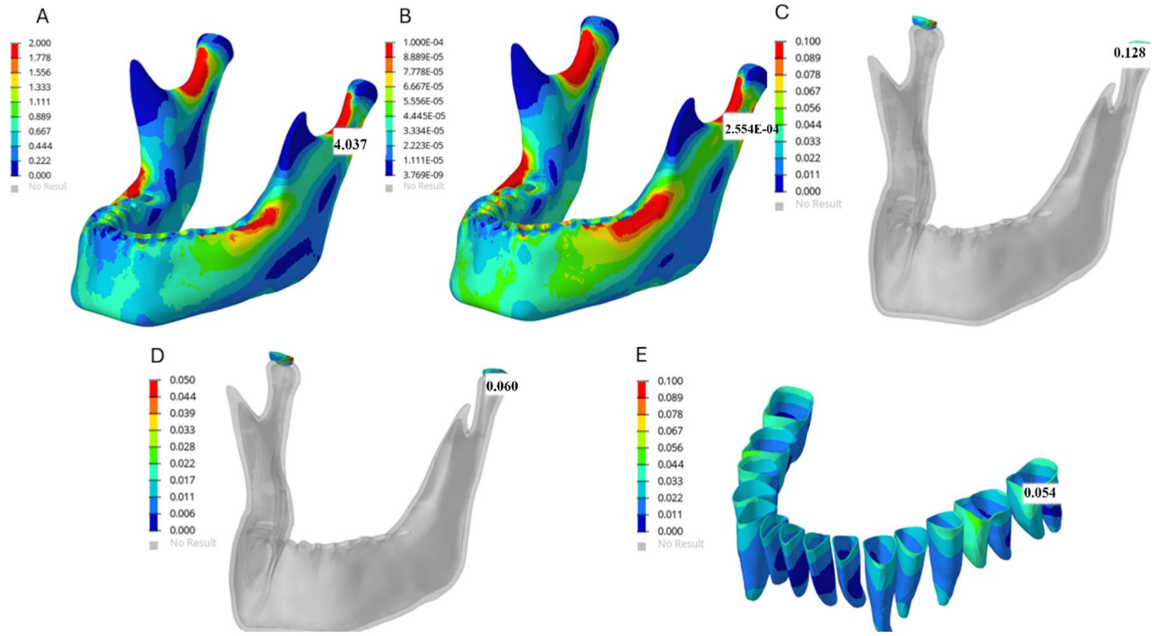

Fig. 14 Protrusive movement in the splint-free (NS) model was evaluated to characterize baseline biomechanical responses. Mandibular von Mises stress and strain distributions are shown in (**a**, **b**), articular disc stress and strain in (**c**, **d**), and periodontal ligament (PDL) stress distribution in (**e**). Load vectors are directed anteriorly, reflecting forward condylar translation and increased incisal loading. This configuration represents the baseline protrusive loading pattern used for comparison with splint-assisted conditions

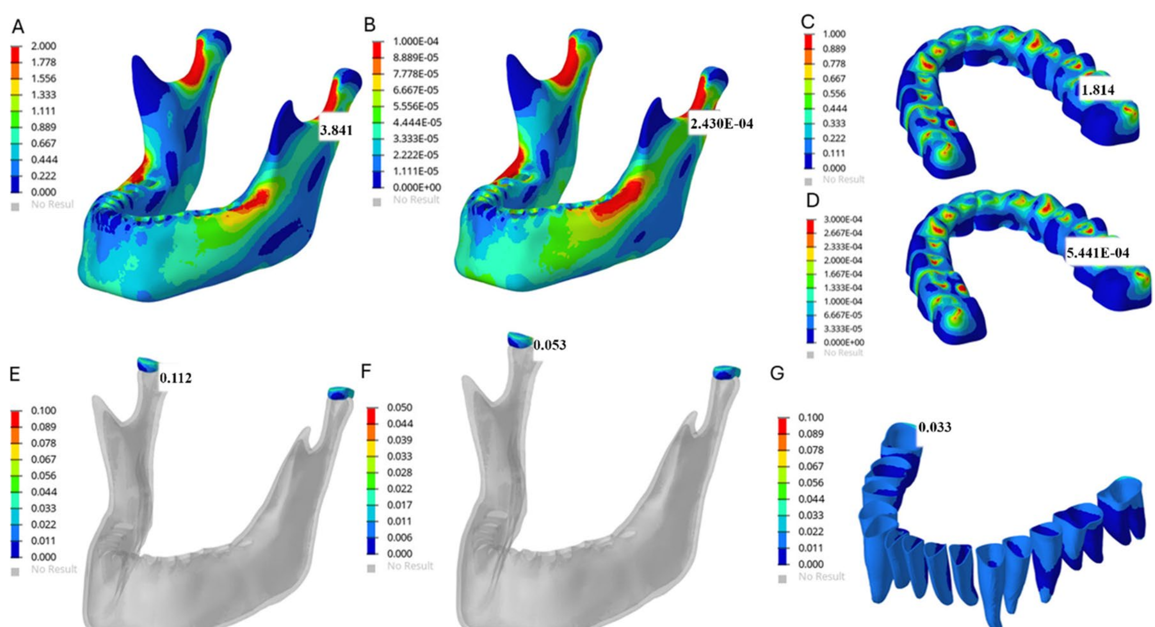

Fig. 15 Protrusive movement in the 3-mm Michigan-type splint (M3) model was evaluated to assess its biomechanical effects. Mandibular stress and strain distributions are shown in (**a**, **b**), and stress and strain within the splint material are illustrated in (**c**, **d**). The articular disc exhibits a central–superior shift in stress and strain (**e**, **f**), while the periodontal ligament (PDL) demonstrates reduced anterior loading (**g**). Compared with the splint-free condition, the M3 splint reduced mandibular and disc stresses and redistributed load toward a more central–superior region of the disc, indicating a more balanced and protective protrusive loading pattern

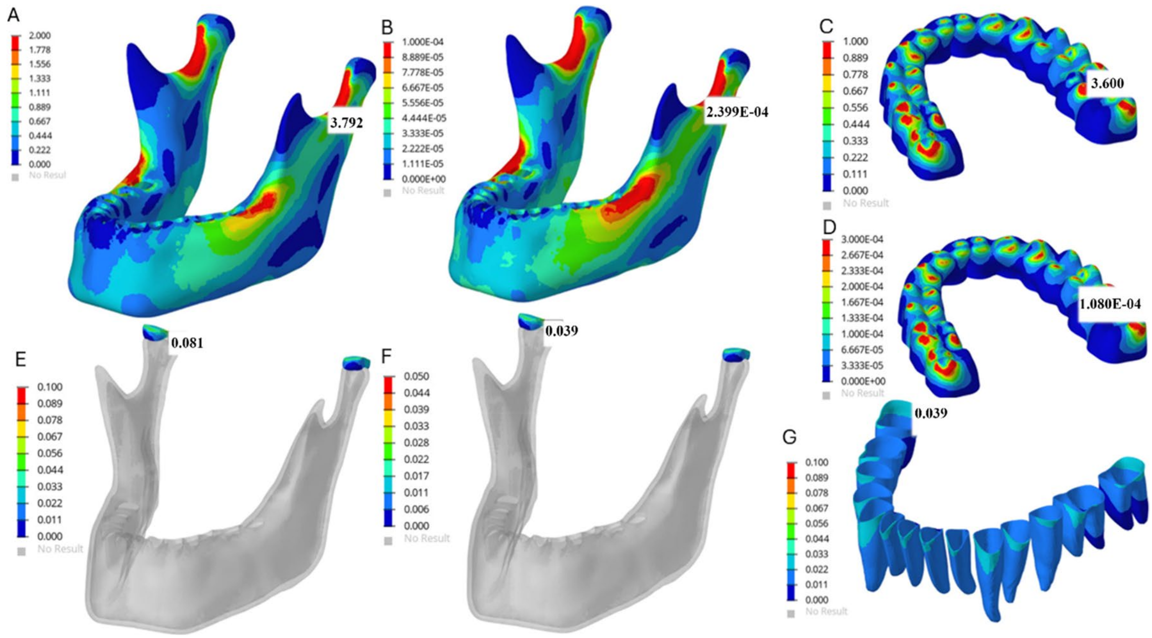

Fig. 16 Protrusive movement in the 3-mm non-permissive splint (NP3) model was evaluated to assess its biomechanical effects. Mandibular von Mises stress and strain distributions are shown in (**a**, **b**), and splint stress and strain are presented in (**c**, **d**). The articular disc exhibits stress and strain concentrated in the posterosuperior region (**e**, **f**), while the periodontal ligament (PDL) shows predominantly posterior stress distribution (**g**). Compared with the splint-free condition, the NP3 splint reduced mandibular and disc stresses and limited anterior disc loading, with stress predominantly confined to the posterosuperior region, indicating a more posteriorly focused load transfer during protrusive movement

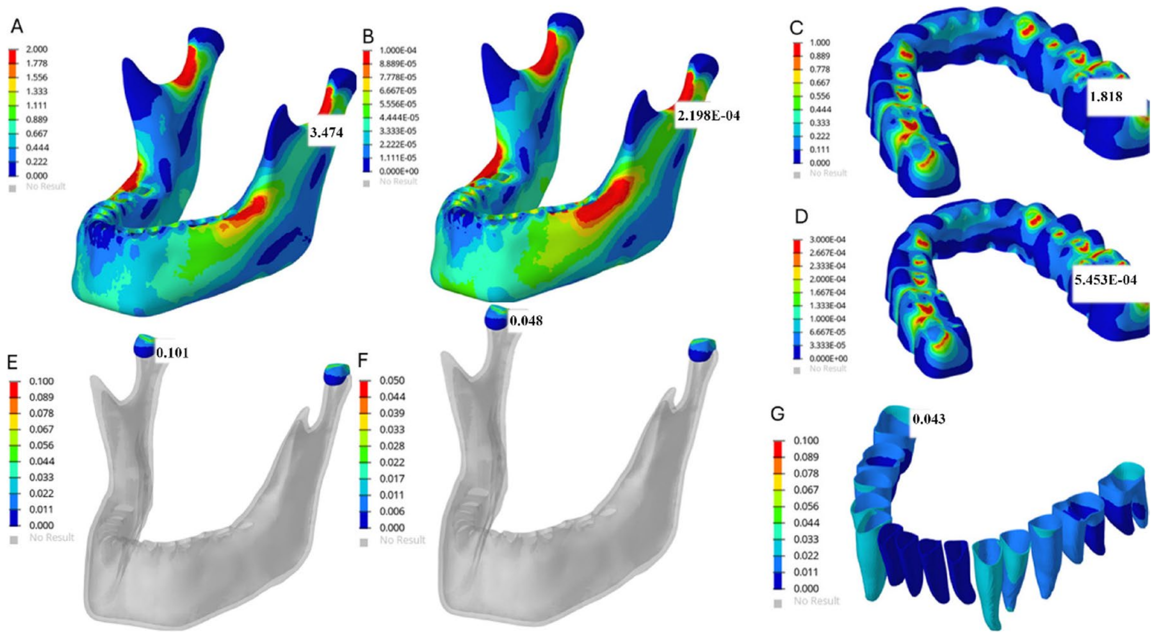

Fig. 17 Protrusive movement in the 5-mm Michigan-type splint (M5) model was evaluated to assess its biomechanical effects. Mandibular von Mises stress and strain distributions are shown in (**a**, **b**), and stress and strain within the splint material are presented in (**c**, **d**). The articular disc exhibits stress and strain concentrated in the central–posterior region (**e**, **f**), while the periodontal ligament (PDL) stress distribution is illustrated in (**g**). Compared with the splint-free model, the M5 splint markedly reduced stress and strain across mandibular, disc, and PDL structures, with minimal anterior loading, indicating an effective redistribution of protrusive forces toward central and posterior regions

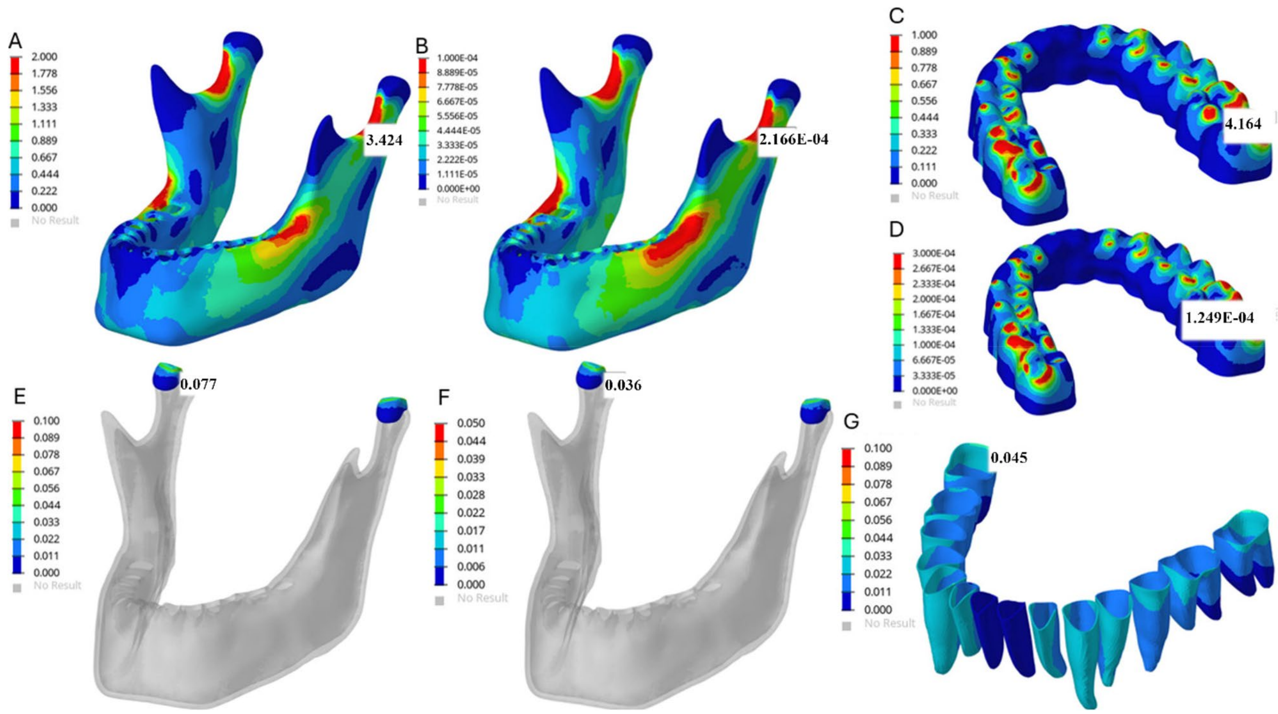

Fig. 18 Protrusive movement in the 5-mm non-permissive splint (NP5) model was evaluated to assess its biomechanical effects. Mandibular stress and strain distributions are shown in (**a**, **b**), and stress and strain on the splint material are presented in (**c**, **d**). The articular disc exhibits stress and strain concentrated in posterior regions with reduced anterosuperior loading (**e**, **f**), while the periodontal ligament (PDL) stress distribution is illustrated in (**g**). The NP5 configuration maintained reduced mandibular stress and further limited disc and PDL loading, with stress predominantly confined to posterior regions, indicating an effective posterior load redistribution during protrusive movement

M3 for all movements: full closure (1.38 MPa), lateral (0.021 MPa), and protrusive (0.033 MPa), (Figs. 13, 11 and 12).

The highest mandibular strain values were observed in NP3 during full closure movement (2.355E–03 MPa), (Fig. 8); and in M3 models during lateral (2.05E–04 MPa) and protrusive (2.430E–04 MPa) movement (Figs. 11 and 12). The lowest mandibular strain values were observed in NP5 for all movements: full closure (2.044E–03 MPa), lateral (1.71E–04 MPa), and protrusive (2.166E–04 MPa), (Figs. 10, 9 and 7). The highest stress values in the splints were observed in NP5 during full closure (1.972E–02 MPa), NP3 during lateral movement (9.52E–04 MPa), and M5 during protrusive movement (5.453E–04 MPa), (Figs. 16, 9 and 18). The lowest strain values in the splints were observed in the NP3 model with full closure (1.123E – 02 MPa) and protrusive movement (1.008E – 04 MPa), (Figs. 8 and 17); and in the M3 model with lateral movement (0.40E – 04 MPa), (Fig. 11).

Discussion

Three hypotheses were tested in this study. The first that splint use would reduce stress and strain in the mandible and TMJ compared with no splint was supported. Splint-free models showed higher mandibular stresses, which decreased markedly after splint application. The second hypothesis was not supported, as non-permissive splints produced equal or lower disc stresses than Michigan designs across all thicknesses. The third that thicker splints would further reduce TMJ stress was only partially confirmed. Increased thickness lowered TMJ stress in non-permissive splints but provided no clear advantage in Michigan splints. These findings indicate that splint design, rather than thickness alone, determines biomechanical performance.

In the NS model, under maximum intercuspation and eccentric movements, the stress distribution pattern corresponded closely to the regions previously reported as common sites of disc perforation and degeneration [3, 33]. In the present finite element analysis, a common finding across all splint types and thicknesses was that stress distribution became more balanced after splint application, and stress concentrations on the articular disc shifted away from the posterior contact regions. Under full intercuspation, Michigan-type splints exhibited a broader superior stress distribution, whereas non-permissive designs redirected loading from the posterosuperior zone toward the anterosuperior transition area, distancing the stress field from posterior contacts. This finding is consistent with biomechanical evidence that occlusal splints can modulate load transmission within the TMJ and redistribute stress away from the posterior band, although most previous studies evaluated these effects under static jaw positions [10]. In the NS model, lateral movement analysis revealed that loading was concentrated exclusively in the posterior region. This localized posterior stress concentration may explain why lateral excursions are often described as the most destructive mandibular movements [6, 12]. With splint use, stress during lateral movement shifted toward a more balanced superior distribution. During protrusive loading, Michigan splints concentrated stress in the central posterior region, whereas non-permissive designs limited anterior guidance and maintained a more posteriorly directed load pattern. To our knowledge, this is the first finite element study to describe the detailed stress distribution pattern of a non-permissive splint during the protrusive phase. Clinical evidence also supports this biomechanical behavior, showing that splint therapy reduces muscle activity and stabilizes condylar position [14, 34]. This effect has been attributed to reduced muscle activity and increased condylar stability, as reported in previous studies [9, 24, 35]. Several clinical studies have reported that occlusal splint therapy reduces symptoms and improves patient comfort and function in individuals with TMD and bruxism [34, 36]. The stress redistribution observed in this analysis is consistent with the physiological adaptations associated with occlusal splint therapy and supports its stabilizing effect on joint loading [5, 18]. In contrast, therapies aimed primarily at limiting masticatory muscle function such as botulinum toxin injections have shown limited efficacy in improving joint mechanics [11, 27].

The second hypothesis was not supported. This may be attributed to the controlled mandibular positioning of non-permissive splints, which may promote a more anterior or antero-inferior disc–condyle relationship and reduce posterior band compression [37]. Consistent with this finding, Kim and Somers demonstrated in their finite element analysis that non-permissive splints reduced condylar stress more effectively than permissive designs under vertical clenching, accompanied by localized stress accumulation within the splint material [8]. The literature suggests that non-permissive appliances may reduce pain and joint sounds in the short term; however, recent meta-analyses report no clear consensus and indicate no significant advantage of ARS over other occlusal splints in pain reduction [7, 21]. In terms of muscle loading, use of the NTI-tss device, classified as a non-permissive appliance, has been shown to produce greater reductions in nocturnal EMG activity than Michigan splints, suggesting an indirect decrease in joint loading [38]. However, directive appliances such as NTI or ARS may lead to persistent occlusal changes with prolonged use and therefore require careful case selection and close follow-up [4, 25]. In the current analysis, non-permissive splints produced greater reductions in TMJ loading across all movement types compared with other splints. This finding highlights their stronger biomechanical influence, confirmed by finite element analysis, which also revealed higher localized stress accumulation within the splint material [23]. Based on these findings, non-permissive designs may provide more effective short-term load redistribution in patients with disc displacement, whereas Michigan type stabilization splints remain a safe and predictable first-line option for myofascial pain dominant cases. Nevertheless, due to the potential risk of occlusal alterations associated with non-permissive splints, their duration of use and follow-up should be carefully managed [20].

Contrary to the third hypothesis, splint thickness showed a nonlinear effect on joint loading. In the present model, increasing splint thickness was accompanied by mandibular rotation. This rotation may have altered the disc–condyle contact area and contributed to the nonlinear stress distribution observed within the TMJ. Increasing thickness from 3 mm to 5 mm slightly but consistently reduced disc stress in the non-permissive splint, whereas the Michigan-type splint showed a plateau pattern, with stress values remaining nearly unchanged. One possible explanation is the redistribution of functional loads within the splinted system. In the present analysis, the 5-mm non-permissive splint reduced mandibular stress but increased stress concentration within the splint, suggesting that occlusal loads may have been redistributed rather than transmitted directly to the mandibular complex.

The prevailing view in the literature is that optimal splint thickness should be individualized according to joint condition and patient characteristics. An MRI-guided randomized controlled trial similarly indicated that thickness requirements differ between disc displacement with and without reduction [15, 16]. Likewise, a finite element analysis of non-reducing anterior disc displacement showed that beyond a certain threshold, increasing splint thickness provides only limited additional reduction in joint stress [13, 26]. Moreover, some studies have shown that excessive splint thickness may paradoxically increase masticatory muscle activity in certain patients [22]. In the present FEA, the 5-mm non-permissive splint reduced mandibular loading but increased stress accumulation in the periodontal structures, whereas the Michigan design showed no additional benefit between 3 and 5 mm. Clinical electromyographic studies have shown that non-permissive appliances such as NTI-type devices can significantly reduce nocturnal jaw-closing muscle activity, suggesting a reduction in the functional loading transmitted to the temporomandibular joint [18, 39]. Consistent with these findings, the present finite element analysis also demonstrated reduced stress levels in the TMJ structures. However, clinical reports have described occlusal alterations and tooth mobility associated with prolonged use of directive splints, indicating that occlusal contact patterns may change. These alterations may redistribute functional loads within the dentition [7, 20, 21]. Therefore, although non-permissive splints may contribute to joint unloading, the resulting concentration of occlusal contacts may increase localized stresses in the periodontal supporting structures, indicating a potential biomechanical trade-off between joint protection and dental loading. These findings highlight the complex, interactive influence of splint thickness on joint and supporting tissues and suggest that clinical management should follow an individualized, stage-specific approach rather than a single fixed thickness. Despite being a comprehensive finite element analysis incorporating multiple mandibular positions and vector-defined muscle forces, this study has several methodological limitations. First, anterior guidance and frictional sliding components of tooth contacts were not modeled, which may limit the representation of anteriorly directed effects of the non-permissive splint. Second, high, localized shear stresses expected during lateral excursions may have been partially dampened due to the kinematic boundary constraints, potentially underrepresenting load accumulation during these movements. Third, although muscle force directions were defined for eccentric movements, their temporal activation sequence was not simulated. In addition, all structures were modeled as linear-elastic and isotropic, excluding the viscoelastic, time-dependent behavior of soft tissues. Analyses were performed under linear static conditions, omitting contact friction, ligament tension, and nonlinear deformation effects. Therefore, while the comparative stress distribution trends observed in this study are considered clinically meaningful, the absolute stress magnitudes should not be interpreted directly as physiological values.

Another limitation of finite element studies is the common assumption that the jawbone is homogeneous. However, the jawbone is structurally heterogeneous and exhibits anisotropic characteristics, which may lead to different stress distributions and densities. Additionally, the friction coefficient at the splint–tooth interface was assumed to be zero, which may not fully reflect clinical conditions. Furthermore, this model represents a controlled virtual simulation and cannot reproduce the naturally varying and multifactorial stresses present in the oral cavity. The model also cannot account for patient variability in anatomy or muscle activation patterns. Finally, the lack of dynamic or fatigue analysis limits the interpretation of these findings for long-term clinical use. Considering these limitations, further experimental and clinical studies are needed to better clarify the biomechanical effects of different splint designs and thicknesses.

Conclusion

Within the limitations of this finite element analysis, the following conclusions can be drawn:

- Occlusal splint use reduced peak stresses in the mandibular bone and TMJ structures compared with the splint-free condition.
- The non-permissive design maintained equal or lower stress levels on the articular disc than the Michigan splint, while producing the lowest mandibular stresses, particularly with increased thickness.
- Increasing splint thickness from 3 mm to 5 mm further decreased mandibular and joint loading in the non-permissive design, whereas this change did not confer a significant biomechanical advantage in the Michigan splint.
- Although non-permissive splints reduced loading on the joint, they generated higher stresses in the periodontal ligament, indicating a potential trade-off between joint protection and tooth or tissue loading.
- Splint design and thickness influence stress distribution in distinct ways; therefore, both the biomechanical profile and patient-specific diagnosis and tolerance should be considered to achieve an individualized, evidence-based approach in clinical practice.

Supplementary Information

The online version contains supplementary material available at https://doi.org/10.1186/s12903-026-08376-6.

Supplementary Material 1

Clinical trial number

Not applicable.

Authors' contributions

Conceptualization, methodology, data curation, formal analysis, visualization, and writing—original draft preparation, B.T.; finite element modeling and software validation, B.T. and E.G.S.; investigation and resources, A.Ç.Ş. and H.A.; review and editing, B.T. and K.K.; supervision, B.T. All authors have read and approved the final version of the manuscript.

Funding

This research received no external funding.

Data availability

The datasets generated and analyzed during the current study are available from the corresponding author on reasonable request.

Declarations

Ethics approval and consent to participate

This study was approved by the Non-Interventional Clinical Research Ethics Committee of the University of Health Sciences, Hamidiye Campus (Date: May 15, 2025; Decision No: 11/33; Project Registration No: 25/444). All procedures were performed in accordance with institutional and national ethical standards.

Competing interests

The authors declare no competing interests.

Received: 25 December 2025 / Accepted: 13 April 2026
Published online: 07 May 2026

References

1. Okeson J. Management of temporomandibular disorders and occlusion. N Y State Dent J. 2003;69:61.
2. Dylina TJ. The basics of occlusal splint therapy. Dent Today. 2002;21:82–7.
3. Machon V, Levorova J, Hirjak D, Drahos M, Foltan R. Temporomandibular joint disc perforation: a retrospective study. Int J Oral Maxillofac Surg. 2017;46:1411–6. https://doi.org/10.1016/j.ijom.2017.05.008.
4. Lukic N, Saxer T, Hou M-Y, Zumbrunn Wojczyńska A, Gallo LM, Colombo V. Short-term effects of NTI-tss and Michigan splint on nocturnal jaw muscle activity: a pilot study. Clin Exp Dent Res. 2021;7:323–30. https://doi.org/10.1002/cre2.371.
5. Beard CC, Clayton JA. Effects of occlusal splint therapy on TMJ dysfunction. J Prosthet Dent. 1980;44:324–35. https://doi.org/10.1016/0022-3913(80)90021-9.
6. Duanmu Z, Liu L, Deng Q, Ren Y, Wang M. Development of a biomechanical model for dynamic occlusal stress analysis. Int J Oral Sci. 2021;13:29. https://doi.org/10.1038/s41368-021-00133-5.
7. Guo Y-N, Cui S-J, Zhou Y-H, Wang X-D. An overview of anterior repositioning splint therapy for disc displacement-related temporomandibular disorders. Curr Med Sci. 2021;41:626–34. https://doi.org/10.1007/s11596-021-2381-7.
8. Kim SSY, Somers M. Finite analysis of temporomandibular joint loading with occlusal splint use. J Int Clin Dent Res Org. 2023;15:23–6. https://doi.org/10.4103/jicdro.jicdro_10_20.
9. Singh D, Landry A, Schmid-Schwap M, Piehslinger E, Gahleitner A, Chen J, et al. Clinical and MRI-based assessment of patients with temporomandibular disorders treated by controlled mandibular repositioning. Diagnostics. 2024;14:572. https://doi.org/10.3390/diagnostics14060572.
10. Porntirit R, Rewthamrongsris P, Assoratgoon I, Osathanon T. Anatomical changes after stabilisation splint therapy: a systematic review and meta-analysis. Int Dent J. 2025;75:100952. https://doi.org/10.1016/j.identj.2025.100952.
11. Gouda KG, Rezkallah SS, Khalil AA. Stabilization splint versus botulinum toxin injection on masticatory muscles activity in patients with temporomandibular disorders: a narrative review. Benha Int J Phys Ther. 2025;3:257–67. https://doi.org/10.21608/bijpt.2025.377234.1084.
12. Del Pérez A, Doblaré M. Finite element analysis of the temporomandibular joint during lateral excursions of the mandible. J Biomech. 2006;39:2153–63. https://doi.org/10.1016/j.jbiomech.2005.06.020.
13. Lin SL, Wu SL, Ko SY, Yen CY, Yang JW. Effect of flat-plane splint vertical thickness on disc displacement without reduction: a retrospective matched-cohort study. J Oral Maxillofac Surg. 2017;75:1627–36. https://doi.org/10.1016/j.joms.2016.12.047.
14. Seiler A, Lukic N, Özcan M, Kazimi M, Kaldas M, Gallo LM, et al. Temporomandibular joint space variation and masticatory muscle activation during clenching with full versus partial covering occlusal splints. Clin Oral Investig. 2024;28:584. https://doi.org/10.1007/s00784-024-05980-0.
15. He J, Ran J, Zheng B, Algahefi A, Liu Y. Finite element analysis of various thickness occlusal stabilization splint therapy on unilateral temporomandibular joint anterior disc displacement without reduction. Am J Orthod Dentofac Orthop. 2022;161:e277–86. https://doi.org/10.1016/j.ajodo.2021.09.011.
16. Sharma J, Banerjee R, Gajbhiye V, Bhoge A, Jaiswal P, Nayak K. Randomized clinical trial to evaluate the effectiveness of different thicknesses of stabilization splints in treating temporomandibular disorder using joint vibration analysis as a novel diagnostic tool. J Indian Prosthodont Soc. 2025;25:210–9. https://doi.org/10.4103/jips.jips_76_25.
17. Al-Moraissi EA, Farea R, Qasem KA, Al-Wadeai MS, Al-Sabahi ME, Al-Iryani GM. Effectiveness of occlusal splint therapy in the management of temporomandibular disorders: network meta-analysis of randomized controlled trials. Int J Oral Maxillofac Surg. 2020;49:1042–56. https://doi.org/10.1016/j.ijom.2020.01.004.
18. Ainoosah S, Farghal AE, Alzemei MS, Saini RS, Gurumurthy V, Quadri SA, et al. Comparative analysis of different types of occlusal splints for the management of sleep bruxism: a systematic review. BMC Oral Health. 2024;24:29. https://doi.org/10.1186/s12903-023-03782-6.
19. Okeson JP. The effects of hard and soft occlusal splints on nocturnal bruxism. J Am Dent Assoc. 1987;114:788–91. https://doi.org/10.14219/jada.archive.1987.0165.
20. Dhar S, Kumar N, Ashrafullah, Dhaded N, Hegde P, Chhabaria Peswani K. Assessing the efficacy of anterior repositioning splints in the management of temporomandibular disc displacement: a systematic review and meta-analysis. Cureus. 2023;15:e47689. https://doi.org/10.7759/cureus.47689.
21. Wang L, Zhang Y, Chen H, Jin C, Shen W, Li Z, et al. The efficacy of anterior repositioning splints in the management of temporomandibular disc displacement: a systematic review and meta-analysis. BMC Oral Health. 2025;25:1267. https://doi.org/10.1186/s12903-025-06379-3.
22. Abekura H, Yokomura M, Sadamori S, Hamada T. The initial effects of occlusal splint vertical thickness on the nocturnal EMG activities of masticatory muscles in subjects with a bruxism habit. Int J Prosthodont. 2008;21:116–20.
23. Gholampour S, Gholampour H, Khanmohammadi H. Finite element analysis of occlusal splint therapy in patients with bruxism. BMC Oral Health. 2019;19:205. https://doi.org/10.1186/s12903-019-0897-z.
24. Riley P, Glenny A-M, Worthington HV, Jacobsen E, Robertson C, Durham J, et al. Oral splints for temporomandibular disorder or bruxism: a systematic review. Br Dent J. 2020;228:191–7. https://doi.org/10.1038/s41415-020-1250-2.
25. Jokstad A. The NTI-tss device may be used successfully in the management of bruxism and TMD. Evid Based Dent. 2009;10:23. https://doi.org/10.1038/sj.ebd.6400635.
26. Hegab AF, Youssef AH, Abd Al Hameed H, Karam KS. MRI-based determination of occlusal splint thickness for temporomandibular joint disk derangement: a randomized controlled clinical trial. Oral Surg Oral Med Oral Pathol Oral Radiol. 2018;125:74–87. https://doi.org/10.1016/j.oooo.2017.09.017.
27. Minston A, Abrahamsson H, Abrahamsson P, Lindfors E, Nohlert E, Ovesson D, et al. Effect on pain following one session of botulinum toxin type A in patients with jaw myalgia: a randomised double-blind controlled multicentre pilot study. J Oral Rehabil. 2025;52:587–96. https://doi.org/10.1111/joor.13915.
28. U.S. National Library of Medicine. The visible human project. 2025. https://www.nlm.nih.gov/research/visible/visible_human.html.
29. Samii M, Draf W, Lang J. Anatomy of the temporomandibular joint. surgery of the skull base: an interdisciplinary approach. Berlin Heidelberg: Springer-; 1989. p. 41–2.
30. Müller-Leisse C, Augthun M, Bauer W, Roth A, Günther RW. Temporomandibular joint morphology and morphometric findings in relation to degree of disk displacement. Comparative magnetic resonance tomography studies. Radiologe. 1997;37:152–8. https://doi.org/10.1007/s001170050188.
31. Moga RA, Buru SM, Olteanu CD. Assessment of the best FEA failure criteria (Part II): Investigation of the biomechanical behavior of dental pulp and apical neuro-vascular bundle in intact and reduced periodontium. Int J Environ Res Public Health. 2022;19:15635. https://doi.org/10.3390/ijerph192315635.
32. Iwasaki LR, Liu H, Gonzalez YM, Marx DB, Nickel JC. Modeling of muscle forces in humans with and without temporomandibular joint disorders. J Oral Rehabil. 2015;42:346–56. https://doi.org/10.1111/joor.12248.
33. Muñoz-Guerra MF, Rodríguez-Campo FJ, Escorial Hernández V, Sánchez-Acedo C, Gil-Díez Usandizaga JL. Temporomandibular joint disc perforation: long-term results after operative arthroscopy. J Oral Maxillofac Surg. 2013;71:667–76. https://doi.org/10.1016/j.joms.2012.12.013.
34. Esteve M, Rosales Leal JI. Effects of occlusal splints on temporomandibular disorders and well-being among fibromyalgia and bruxism patients: a quasi-experimental study. Appl Sci. 2025;15:4465. https://doi.org/10.3390/app15084465.
35. Ferrario VF, Sforza C, Tartaglia GM, Dellavia C. Immediate effect of a stabilization splint on masticatory muscle activity in temporomandibular disorder patients. J Oral Rehabil. 2002;29:810–5. https://doi.org/10.1046/j.1365-2842.2002.00927.x.
36. Loan HK, Hai HV, Tung NA, Phu NM, Duc NM. Treatment outcomes of temporomandibular disorders using stabilization splint supported by the T-scan system. Eur J Dent. 2025. https://doi.org/10.1055/s-0045-1809915.
37. Song J, Xiao Q, Cen X. [Effect of disc morphological features and disc-condyle angles on conservative treatment for anterior disc displacement with reduction]. Hua Xi Kou Qiang Yi Xue Za Zhi. 2025;43:406–15. https://doi.org/10.7518/hxkq.2025.2024313.
38. Rampal S, Shreenidhi H, Shrivastava M, Singh AP, Reena R, Kumar SD. Exploring the use of machine learning techniques for enhancing real-time data access. In: proceedings of the 3rd international conference on Smart

Generation Computing, Communication and Networking (SMART GENCON). IEEE. 2023;591:02002.
39. Baad-Hansen L, Jadidi F, Castrillon E, Thomsen PB, Svensson P. Effect of a nociceptive trigeminal inhibition splint on jaw-muscle activity in sleep bruxism. J Oral Rehabil. 2007;34:105–11. https://doi.org/10.1111/j.1365-2842.2006.01658.x.

Publisher's note